Supporting Information

Atomic-Level Localization of π-Electrons in Defect Engineered Tri-s-triazine Units for Increased Photocatalytic Hydrogen Generation of Polymeric Carbon Nitride

Mengqi Xue,[a†] Daochuan Jiang,[a†] Haiwei Du,[a] Zhongjun Li,[b,*] Hong Bi,[a] and Yupeng Yuan[a,c,d]*

[a] *School of Chemistry and Chemical Engineering, Anhui Province Key Laboratory of Chemistry for Inorganic/Organic Hybrid Functionalized Materials, Anhui University, Hefei, 230601, P. R. China.*

[b] *School of Electronic Science and Applied Physics, Hefei University of Technology, Hefei 230009, P. R. China*

[c] *Key Laboratory of Structure and Functional Regulation of Hybrid Materials (Anhui University), Ministry of Education, Hefei, 230601, P. R. China*

[d] *Energy Materials and Devices Key Lab of Anhui Province for Photoelectric Conversion, Hefei, 230601, P. R. China*

*Corresponding authors

Emails: yupengyuan@ahu.edu.cn (Y. Yuan), and zjli@hfut.edu.cn (Z. Li)
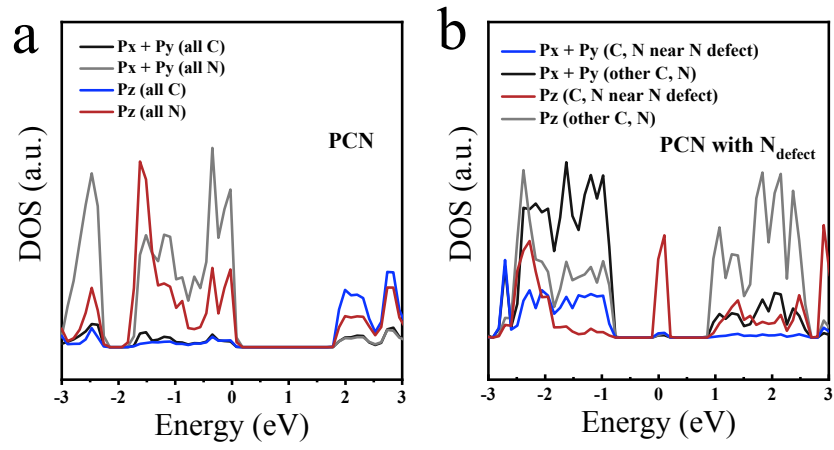
[†] These authors contribute equally to this work.

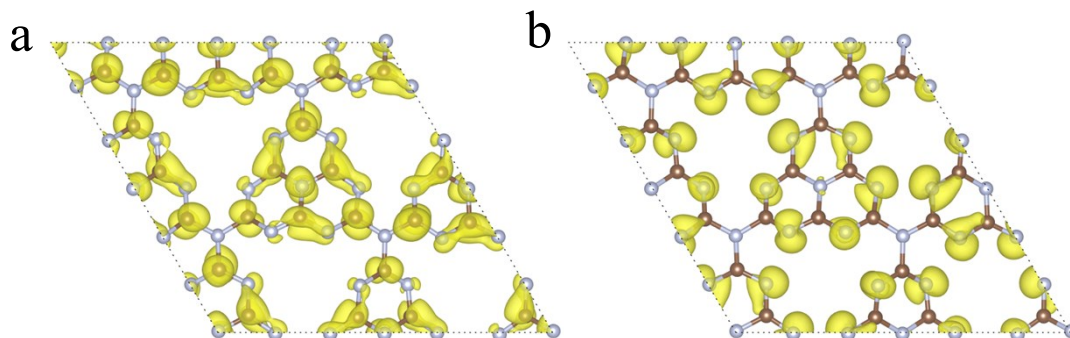**Figure S1**. DOS for PCN (a) and N_{defect} engineered PCN (b).

Figure S2. The charge density distributions of LUMO (a) and HOMO (b) orbitals for
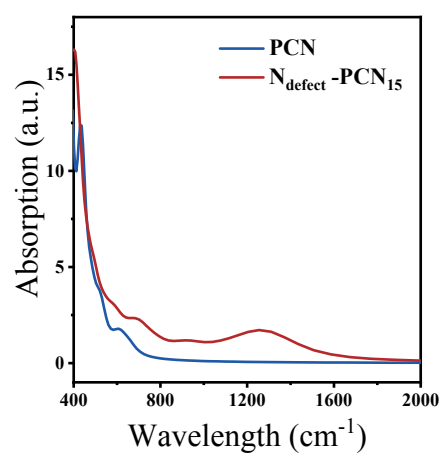
pristine PCN.

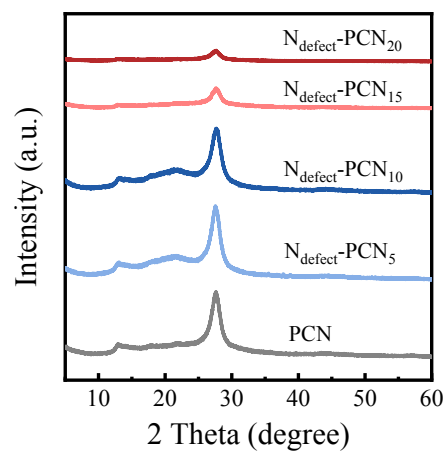**Figure S3**. Calculated absorption coefficients for PCN and PCN with N defect.
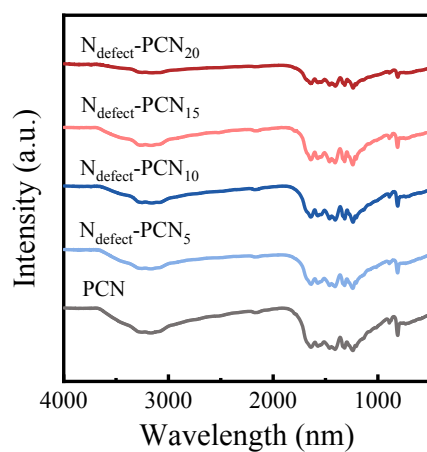
Figure S4. XRD patterns of different samples.
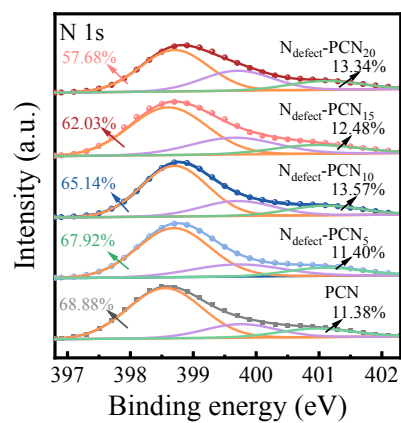
Figure S5. FTIR spectra of different samples.

Figure S6. high-resolution XPS spectra of N 1s for PCN, N_{defect}-PCN$_5$, N_{defect}-PCN$_{10}$, N_{defect}-PCN$_{15}$ and N_{defect}-PCN$_{20}$.
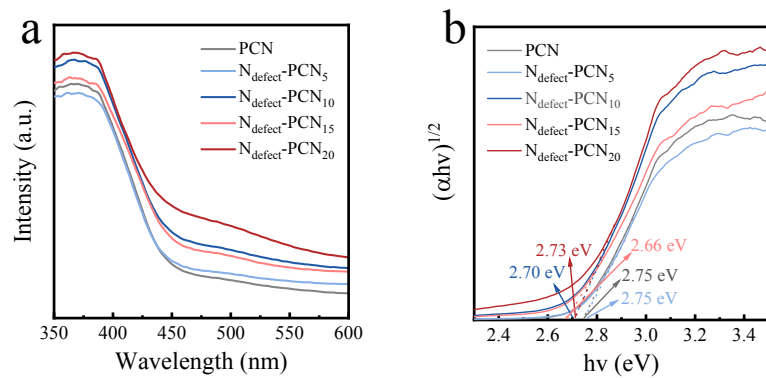
Figure S7. The UV-vis spectra (a) and Tauc plots of PCN, N_{defect}-PCN$_5$, N_{defect}-PCN$_{10}$, N_{defect}-PCN$_{15}$, and N_{defect}-PCN$_{20}$.
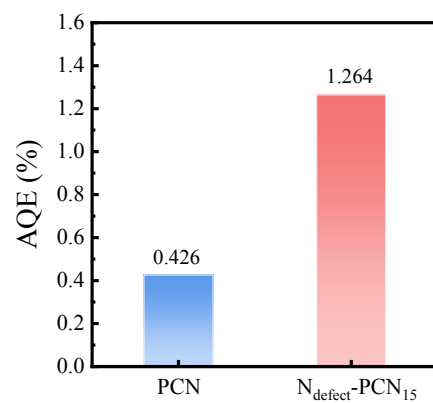
Figure S8. The AQE of PCN and PCN with N defect.
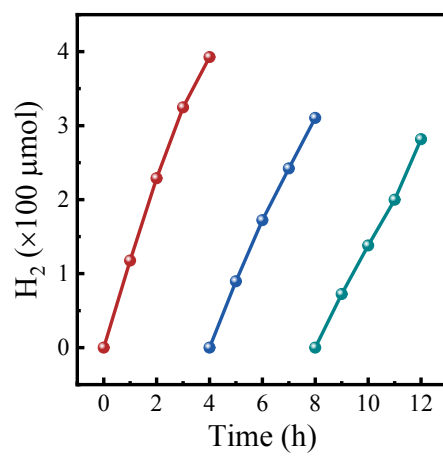
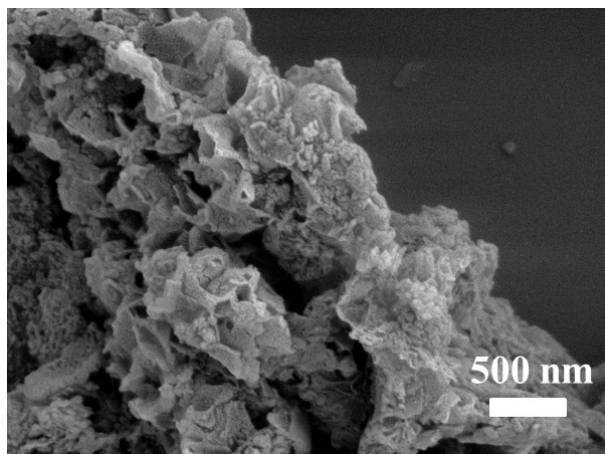**Figure S9**. Stability test under consecutive runs of N_{defect} -PCN$_{15}$.

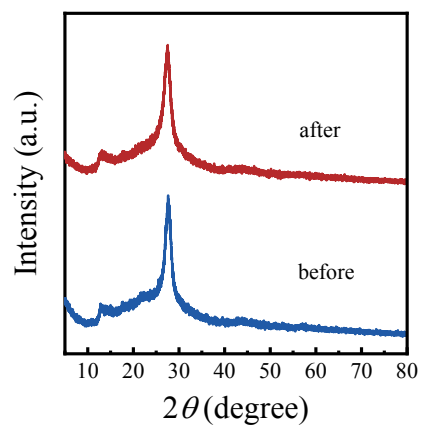**Figure S10**. SEM image of N_{defect}-PCN$_{15}$ after stability test.

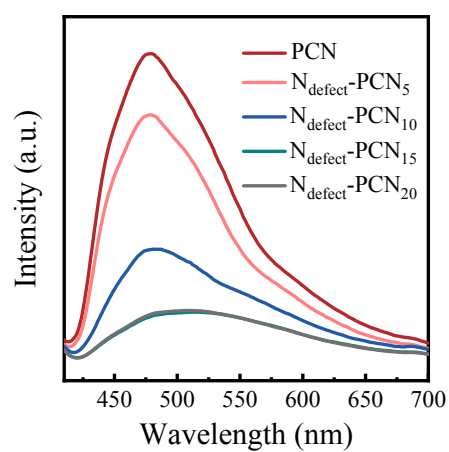**Figure S11.** XRD patterns of N_{defect}-PCN$_{15}$ before and after reaction.

Figure S12. Steady state PL spectra of different samples.